Chemistry–A European Journal
Research Article
doi.org/10.1002/chem.202301762
Chemistry Europe
European Chemical Societies Publishing
www.chemeurj.org

Special Collection

Graphene Oxide Nanosheets Hamper Glutamate Mediated Excitotoxicity and Protect Neuronal Survival In An *In vitro* Stroke Model

Lorenza Tortella[+],[a] Irene Santini[+],[a] Neus Lozano,[b] Kostas Kostarelos,[b, c] Giada Cellot,*[a] and Laura Ballerini*[a]

Dedicated to Professor Maurizio Prato on the occasion of his retirement.

Small graphene oxide (s-GO) nanosheets reversibly downregulate central nervous system (CNS) excitatory synapses, with potential developments as future therapeutic tools to treat neuro-disorders characterized by altered glutamatergic transmission. Excitotoxicity, namely cell death triggered by exceeding ambient glutamate fueling over-activation of excitatory synapses, is a pathogenic mechanism shared by several neural diseases, from ischemic stroke to neurodegenerative disorders. In this work, CNS cultures were exposed to oxygen-glucose deprivation (OGD) to mimic ischemic stroke *in vitro*, and it is show that the delivery of s-GO following OGD, during the endogenous build-up of secondary damage and excitotoxicity, improved neuronal survival. In a different paradigm, excitotoxicity cell damage was reproduced through exogenous glutamate application, and s-GO co-treatment protected neuronal integrity, potentially by directly downregulating the synaptic over-activation brought about by exogenous glutamate. This proof-of-concept study suggests that s-GO may find novel applications in therapeutic developments for treating excitotoxicity-driven neural cell death.

Introduction

During the last decade, graphene related materials (GRMs) were increasingly exploited in biomedical applications[1–3] to promote alternative therapeutic approaches and to cure brain disorders.[4,5] More specifically, the reduced dimensions of GRMs, matching those of the smallest CNS functional units, such as the sub-cellular structures composing synapses,[6–8] prompted their use to manipulate neuronal function during brain pathologies.[9]

One of the most promising GRMs are graphene oxide nanosheets with small lateral size (< 500 nm, s-GO). This nanomaterial has been reported both *in vitro* and *in vivo* to modulate specifically and selectively excitatory synapses,[10–12] by interfering with the presynaptic release of glutamate, leading to downregulation of glutamatergic synaptic transmission with no impact on neuronal viability.[12,13] Recently, this ability was applied to a rat model of anxiety disorder, in which symptoms arose from a pathological glutamatergic over-signaling in the amygdala. A single *intrathecal* injection of s-GO delivered in the rodent during the disease consolidation normalized the amygdala glutamatergic transmission and anxiety related behaviors.[14]

Although this study supported the s-GO therapeutic value in a specific disorder, it is still underexplored whether s-GO could find a large-scale application for treating other neurological diseases characterized by aberrant glutamatergic signaling. Since glutamate mediated excitotoxicity is a feature shared by the pathogenesis of various brain maladies, ranging from ischemic stroke or brain injury to the degenerative Parkinson's and Alzheimer's diseases,[15] it is relevant to explore the use of s-GO to hinder excitotoxicity, thus preventing its downstream pathological outcomes.

In this work, we investigated the impact of s-GO treatments on excitotoxicity by using an *in vitro* model of ischemic stroke. This is a pathological condition where brain OGD, typically originating from the blockage of a brain artery,[16] due to energy supply disruption and related membrane depolarization, causes an exceeding release of glutamate from pre-synaptic terminals,[17] that induces, as secondary damage, a glutamate

[a] L. Tortella,[+] I. Santini,[+] Dr. G. Cellot, Prof. L. Ballerini
Neuroscience Area
International School for Advanced Studies (SISSA/ISAS)
Via Bonomea 265, 34136 Trieste (Italy)
E-mail: cellot@sissa.it
laura.ballerini@sissa.it
[b] Dr. N. Lozano, Prof. K. Kostarelos
Catalan Institute of Nanoscience and Nanotechnology (ICN2)
CSIC and BIST
Campus UAB, Bellaterra, 08193 Barcelona (Spain)
[c] Prof. K. Kostarelos
Nanomedicine Lab, and Faculty of Biology, Medicine & Health, The National Graphene Institute
University of Manchester
Manchester, M13 9PL (United Kingdom)
[+] These authors contributed equally to this work.

Supporting information for this article is available on the WWW under https://doi.org/10.1002/chem.202301762

This article is part of a joint Special Collection in honor of Maurizio Prato.

mediated excitotoxicity leading to neuroinflammation[18] and augmenting cell death.[19]

By exposing dissociated CNS cells to *in vitro* OGD and assessing cell death through propidium iodide (PI) based assay and immunofluorescence, we found that the application of s-GO during the secondary damage preserved cell viability, increasing specifically neuronal survival. To better characterize the interaction between s-GO and neurons during excitotoxic secondary damage, we induced cell insult by direct administration of exogenous glutamate to cultures.[20] When s-GO was co-applied with the exogenous neurotransmitter, cell death was prevented and loss in neuronal integrity largely decreased. Supported also by our electrophysiological experiments, we propose that s-GO, through a downregulation of the exceeding glutamatergic transmission, effectively protect neurons. Our results highlight the role of s-GO in blocking upstream excitotoxicity, thus extending the therapeutic applicability of the nanomaterial to the treatment of several neuro-disorders characterized by aberrant glutamatergic signaling.

Results and Discussion

s-GO reverts OGD-induced cell death in ischemic stroke model in vitro

The s-GO material used in this work was synthesized following the protocol already reported[21] and was characterized extensively in our previous publications.[12,13,22] As reported in Figure 1, the specific s-GO batch used here was 1–2 nm thick (1–2 layers) with a lateral dimension ranged from 100 to 500 nm (Figure 1).

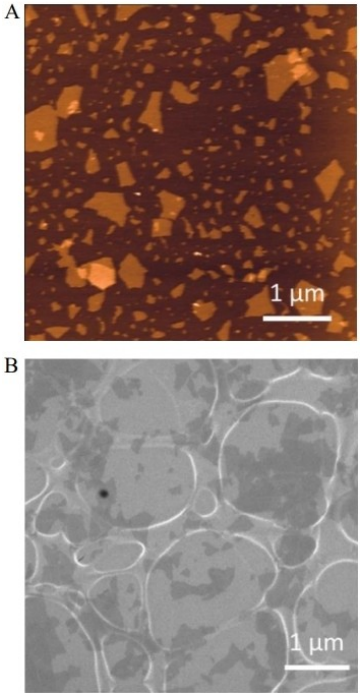

Figure 1. Structural and morphological characterization of s-GO nanosheets. (A) Height atomic force microscopy image (dimension: 5×5). (B) Scanning electron microscopy micrograph.

To explore the potential activity by s-GO in counteracting brain excitotoxicity, we used an *in vitro* model of ischemic stroke, that mimicked the lack of energy dependent glutamate-induced excitotoxicity and the resulting cell death observed in the nervous tissue following acute ischemia *in vivo*.[23,24] To this aim, dissociated hippocampal cultures at the second week of differentiation *in vitro* were treated for 1 hour with an OGD procedure consisting in the exposure to a medium deprived of glucose (OGD solution) in hypoxic atmosphere (see Experimental section and Figure 2A). We selected a duration of the treatment which, according to the literature, enables reproducing a mild cell damage.[25,26] Control cultures were not exposed to changes in glucose and oxygen concentrations. Immediately after the insult, the OGD solution was replaced with culturing medium and cultures were analyzed at different time points.

Due to energy unbalance, OGD leads first to a depolarization of neuronal cell membrane[24,27] that in turn induces a massive release of glutamate neurotransmitter from the presynaptic site of synapses.[28,29] The released glutamate binds and persistently activates its receptors on postsynaptic membranes, depolarizing neurons and escalating the pathogenic cascade leading to cell damage and death.[30,31]

To demonstrate that in our *in vitro* model of ischemic stroke cell damage following OGD was dependent on exceeding glutamatergic signaling, we used ionotropic receptors (GlutRs) antagonists to prevent cell death. Cultures were incubated during OGD and for the following 24 hours with CNQX (10 μM), kynurenic acid (500 μM) and AP-V (25 μM), to block glutamatergic AMPA, kainate and NMDA glutamate receptors respectively, while cell death was quantified after 48 hours from OGD through a PI based assay (Figure 2 A, B). PI is a cell membrane impermeable nucleic acid intercalating fluorescent dye, which labels selectively the nuclei of cells with damaged membrane, namely necrotic cells,[32] while the membrane permeable nuclear marker NucBlue (Hoechst 33342) was exploited to mark all nuclei present in the culture.

Figure 2B shows representative confocal images of cultures that were co-labelled with PI (in red) and NucBlue (in blue). The total number of NucBlue positive cells/field remained constant among the different experimental conditions (see the Experimental section). However, upon OGD, PI positive-damaged cells were increased, while remained similar to the control level when protected by GlutRs antagonists. The percentage of PI necrotic cells (calculated on the total number of NucBlue positive cells) was $27 \pm 1\%$ for controls, $39 \pm 1\%$ for OGD treated cultures and $28 \pm 2\%$ for OGD + GlutRs antagonists treated ones (bar plot in Figure 2C) and differences were statistically significant (control vs OGD and OGD vs OGD + GlutRs antagonists, $P < 0.05$).

Thus, OGD (1 hour) mimicked a moderate ischemic stress with a mild cell death, entirely mediated by glutamate dependent excitotoxicity. s-GO was shown to inhibit pre-synaptic release of glutamate in the CNS,[12,13] thus we investigated s-GO ability to hamper the exceeding glutamate release and to reduce the OGD excitotoxicity. To this aim, we applied the

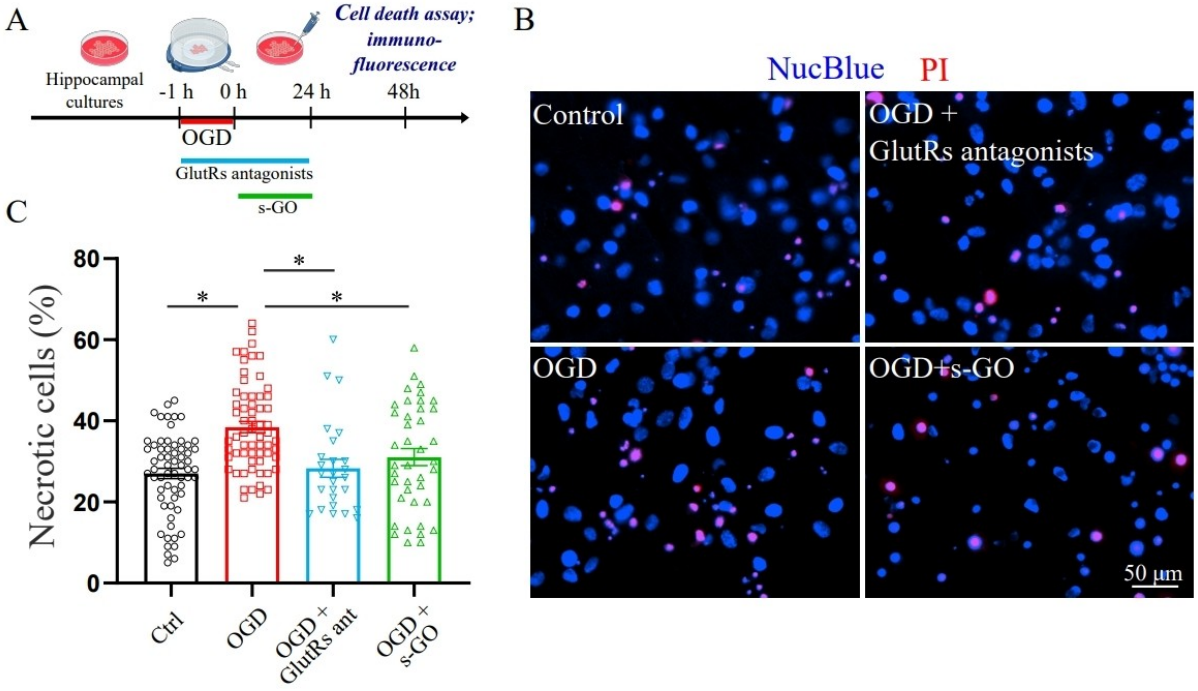

Figure 2. s-GO exerts a protective effect against secondary excitotoxic cell death in an *in vitro* model of ischemic stroke. (A) Schematic representation of the experimental protocol. To induce ischemia in hippocampal cultures, culturing medium (depicted in pink) was replaced with an OGD solution deprived of glucose (in white), and cultures were exposed in a hypoxic chamber to 95% N_2 and 5% CO_2 for 1 hours (red line). After the treatment, cultures were perfused with the initial culturing medium and re-exposed to an O_2 enriched atmosphere. GlutRs antagonists (10 μM of CNQX, 500 μM of kynurenic acid and 25 μM of AP-V) were applied during OGD (in OGD solution, for 1 hour) and after it (in culturing medium, for 24 hours, light blue line). In a different set of samples, s-GO (10 μg/mL) was administered after OGD (in culturing medium, for 24 hours, green line). 48 hours after OGD, cultures were undergone to PI-based cell death assay and immunofluorescence. (B) Magnifications of representative fluorescence microscopy images obtained from cultures (untreated control, OGD, OGD + GlutRs antagonists and OGD + s-GO) undergone to PI based assay. In blue and red cell nuclei stained for NucBlue and PI, respectively. Note that the increment in cell death observed upon OGD was reverted by either GlutRs antagonists or s-GO applications. Scale bar 50 μm. (C) Bar plots showing the percentage of necrotic cells in the different conditions. Data are reported as mean ± SEM, while dots superimposed to the bars correspond to the single field values. N = 63 fields for control and OGD cultures each, N = 26 fields for OGD + GlutR antagonists treated samples and N = 40 fields for OGD + s-GO treated samples, *$P < 0.05$.

nanomaterial at a concentration of 10 μg/mL immediately after OGD and for the following 24 hours (in culturing medium). The timeline of this application was chosen to mimic a possible therapeutic intervention, following ischemic stroke. The concentration of s-GO used was in the range of that reported in literature for inducing modulatory synaptic effects without affecting cell survival in dissociated cultures.[10,14] In s-GO treated OGD cultures, we observed a statistically significant reduction in the amounts of necrotic cells (31 ± 2%, $P < 0.05$) respect to that of the untreated OGD cultures (Figure 2 B,C).

Similarly to GlutRs antagonists treatment, the application of s-GO exerted a protective effect, decreasing the amount of dying cells.

In OGD cultures s-GO promotes neuronal survival without affecting glial cells

After *in vivo* ischemic stroke neurons are the most vulnerable phenotypes to OGD damage, while glial involvement is observed only at a later stage.[33] We investigated the nature of the OGD necrotic cells, to identify which cellular phenotype was preserved by the s-GO treatment.

48 hours after OGD, in the presence or absence of s-GO (24 hours; sketched in Figure 2A), cultures were fixed and immuno-stained with antibodies against the post mitotic neuronal marker NeuN[34] (in grey, Figure 3A) or with the glial fibrillary acidic protein (GFAP, in green, Figure 3B), labelling astrocytic cytoskeleton,[35] while nuclei were stained with DAPI[36] (in blue). Immunofluorescence microscopy revealed that cells dying due to OGD were neurons, as their number decreased in a statistically significant manner ($P < 0.05$) from 24 ± 1 neurons/field in control to 19 ± 1 neurons/field in OGD treated samples (bar plot in Figure 3C). No changes in glial cells densities were observed between the two conditions (16 ± 1 glial cells/field in control and 16 ± 1 glial cells/field in OGD treated samples; bar plot in Figure 3D; $P > 0.05$), indicating the lack of glial death or proliferation due to neuroinflammation.[37] s-GO prevents the OGD reduction in healthy neurons (24 ± 2 neurons/field), which remained similar to that of control cultures (Figure 3C, OGD vs OGD + s-GO, $P < 0.05$), while the amount of glial cells was not modified (14 ± 1 glial cells/field in OGD + s-GO treated samples, Figure 3D, $P > 0.05$). When measured in terms of GFAP intensity, indicative of glial over-reactivity,[38] all cultures displayed similar values (403 ± 8 arbitrary unit, a.u., in control, 434 ± 14 a.u. in

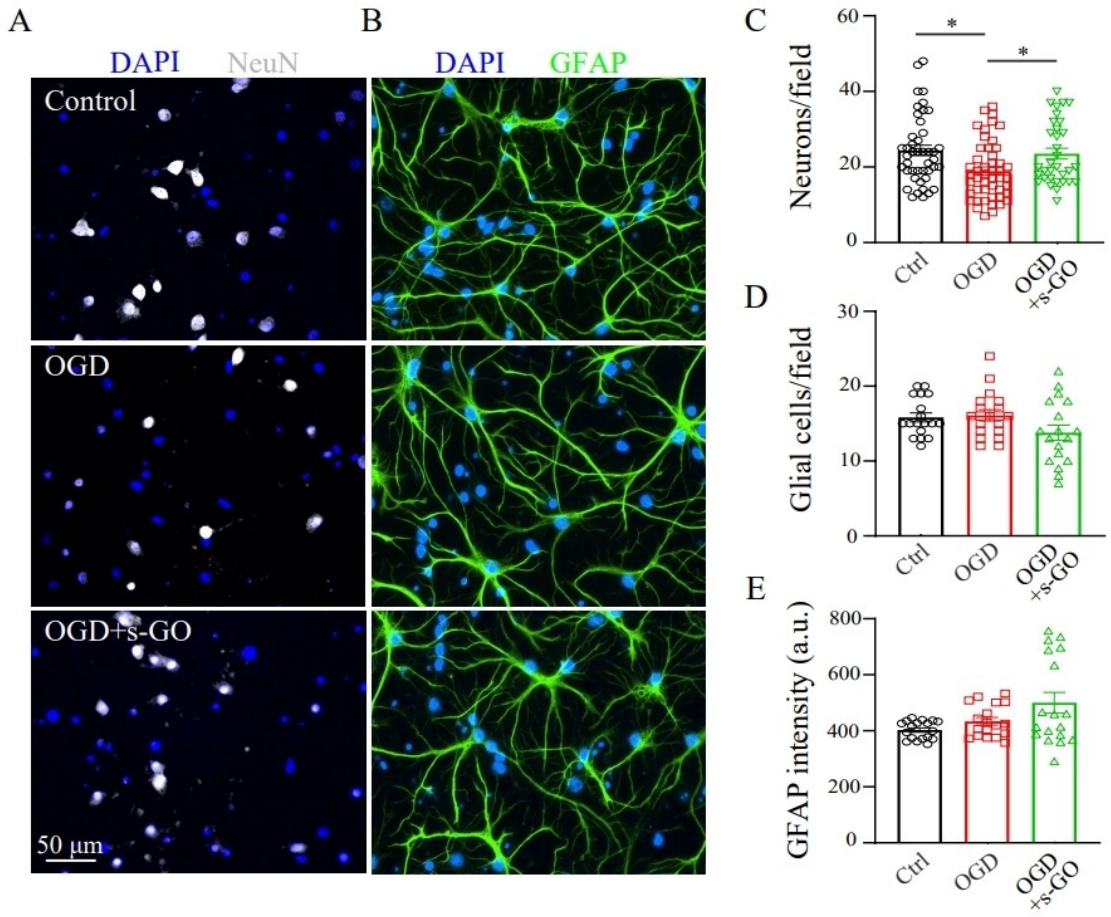

Figure 3. s-GO protects selectively neuronal survival after *in vitro* ischemia. (A-B) Magnifications of representative confocal microscopy images obtained from cultures in control condition and exposed to OGD with or without s-GO post-incubation (10 μg/mL), immunostained for the neuronal and glial markers NeuN (in grey, A) or GFAP (in green, B). In blue cell nuclei staining for DAPI. Note that OGD induced a decrease in the number of neurons that was restored by s-GO treatment, while glial cells were unaffected. Scale bar 50 μm. Bar plots showing the number of neurons (C), the number of GFAP-positive glial cells (D) and the mean GFAP fluorescence intensity (E). Data are reported as mean ± SEM, while dots superimposed to the bars correspond to the single field values. For NeuN staining, N = 44 fields for control, N = 48 fields for OGD treated samples, N = 33 fields for OGD + s-GO treated samples; for GFAP staining, N = 18 fields for each condition; *$P < 0.05$.

OGD treated samples, 500 ± 37 a.u. in OGD + s-GO treated samples; Figure 3E, $P > 0.05$).

This analysis strongly suggested that, at least at the considered time point (48 hours), in OGD cultures no pathological hallmarks could be detected in this cell population.

s-GO protects hippocampal cells from necrosis induced by exogenous glutamate application

To support the glutamatergic pathway and excitotoxicity as the pathogenic mechanisms targeted by s-GO in OGD, we used a simplified *in vitro* model of glutamate-induced excitotoxicity, where dissociated hippocampal cultures were treated directly for 30 minutes with a high concentration of glutamate (40 μM in culturing medium).[20] The application of the exogenous neurotransmitter activates GlutRs, inducing cell depolarization and the release of further, endogenous, glutamate, responsible for a pathogenic loop sustaining excitotoxicity,[39,40] that mimics the processes undergoing during the secondary damage to OGD.

In a group of glutamate (30 min) treated cultures we co-applied s-GO (10 μg/mL). After 30 minutes of incubation, the culturing medium was replaced with a fresh one and, 24 hours later, cell death was evaluated through PI based assay (Figure 4A). Control cultures were exposed neither to glutamate, nor to s-GO. In Figure 4B, PI (in red) and NucBlue (in blue) co-labeled cultures are shown with an enhanced percentage of necrotic cells (28 ± 3%) in glutamate treated samples when compared to controls (14 ± 1%), an effect prevented by s-GO (16 ± 1%; Figure 4C). The differences were statistically significant (for control vs glutamate and glutamate vs glutamate + sGO, $P < 0.05$). We measured no differences in NucBlue positive cells densities among all treatments (see Experimental section). In addition, when cultures were analyzed for mitochondria damage through MitoTracker Red CM–XRos labelling, a similar protective effect of the nanomaterial was detected (Supplementary Figure S1).

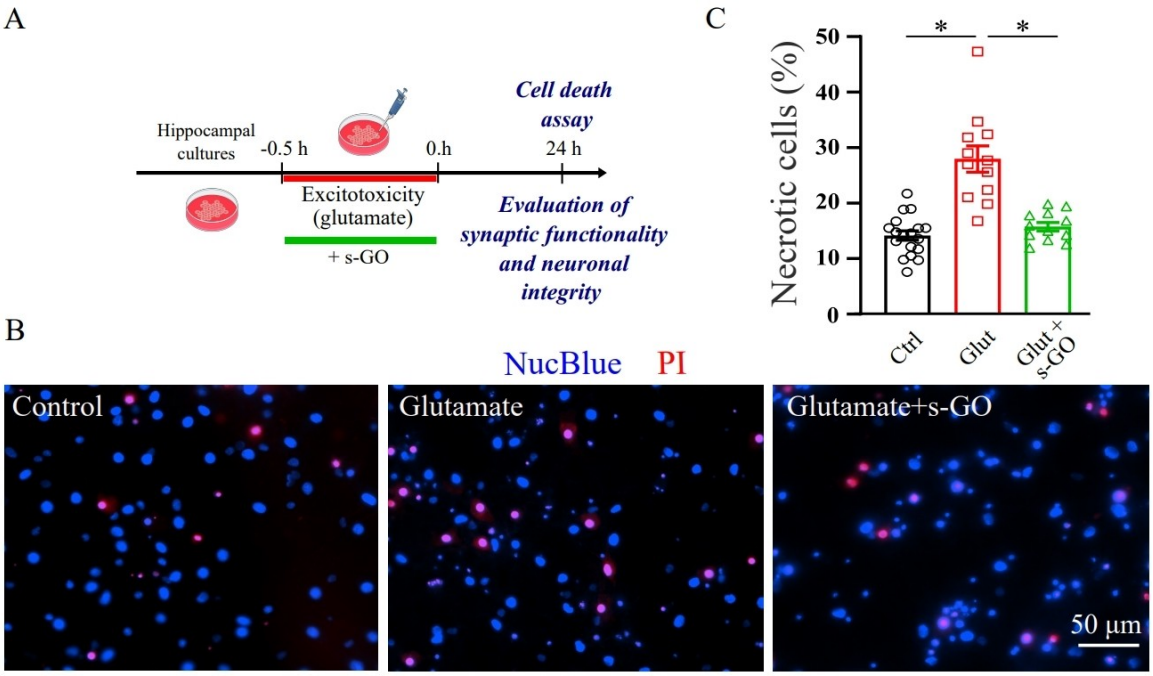

Figure 4. s-GO prevents cell death upon primary excitotoxic insult induced by glutamate application. (A) Schematic representation of the experimental protocol. To induce direct excitotoxicity in hippocampal cultures, culturing medium was added with glutamate (40 μM, red line) for 30 minutes, with or without s-GO (10 μg/mL, green line). 24 hours after the excitotoxic insult, cultures underwent to PI-based cell death assay, electrophysiological recording to assess synaptic functionality and immunofluorescence to measure cell integrity. (B) Representative magnifications of confocal microscopy images in control, glutamate-treated and glutamate + s-GO treated cultures, co-stained for PI (in red) and NucBlue (in blue). Note that the glutamate induced increase in cell death was reverted by s-GO co-treatment. Scale bar 50 μm. (C) Bar plots showing the percentage of necrotic cells in the different conditions. Data are reported as mean ± SEM, while dots superimposed to the bars correspond to the single field values. N = 18 fields for control, N = 12 fields for glutamate and glutamate + s-GO treated samples each, *$P < 0.05$.

These results showed that the exogenous glutamate exposure triggered excitotoxicity and, as in OGD, s-GO protected brain cells from death.

s-GO protects neuronal survival and neurites integrity during excitotoxicity

In the next set of experiments, we used the glutamate-induced excitotoxicity paradigm to further address s-GO protective activity. s-GO was reported to modulate glutamate release from presynaptic terminals[10,12] leading to down regulation of synaptic activity.[10,13,14] Based on these reports, we hypothesized that, s-GO, by inhibiting glutamate release and synaptic activity de-potentiated the excitotoxicity escalation, interrupting the vicious circle, which fuels excitotoxic damage up to neuron death. We used single cell patch clamp recordings to monitor spontaneous synaptic activity after glutamate insult, in cultures co-treated or not with s-GO (10 μg/mL; Figure 4A).

Figure 5A depicts exemplificative current recordings (voltage clamp mode; 24 hours after treatments). The recorded neurons (with comparable membrane passive properties, see Experimental section) displayed spontaneous postsynaptic currents (sPSCs) activated by the release of neurotransmitters from the surrounding neuronal network, mostly of glutamatergic nature in our cultures (see Experimental section). sPSCs frequency depends on neuronal excitability and on the synaptic network size (e.g. smaller networks show less activity[41]) and sPSCs analysis allows to assess whether synapses supported efficiently inter neuronal communication via neurotransmitter release.[42] We observed in glutamate treated cultures a statistically significant ($P < 0.05$) reduction in sPSCs frequency respect to the untreated control (from 7 ± 1.1 Hz to 2.8 ± 0.8 Hz), with no changes in sPSCs amplitude (84.6 ± 9.6 pA and 77 ± 8.6 pA, control and glutamate, respectively; Figure 5B,C). Upon induction of excitotoxicity, the loss of neurons by induced cell death (see Figure 4B,C), results in a neuronal network of smaller size, namely composed by a reduced number of cells respect to control. In cultures co-treated with glutamate and s-GO, we observed a similar reduction in sPSCs frequency (2.4 ± 0.5 Hz, control vs glutamate + s-GO), with no changes in sPSCs amplitude (71.5 ± 9.7 pA; Figure 5B,C). However, when cultures were exposed to glutamate together with s-GO no increased cell death was observed (see Figure 4B,C). Since the size of control and glutamate + s-GO networks were similar, given that s-GO does not affect neuronal excitability,[14] the observed decrease in synaptic activity should reflect a downregulation of synaptic transmission mediated by s-GO[10,12,13,14] more than a reduction in neuronal firing activity.

In a separated set of experiments, we applied s-GO (10 μg/mL) for 30 minutes to control cultures. Similarly to cultures co-incubated with glutamate + s-GO, when recording spontaneous

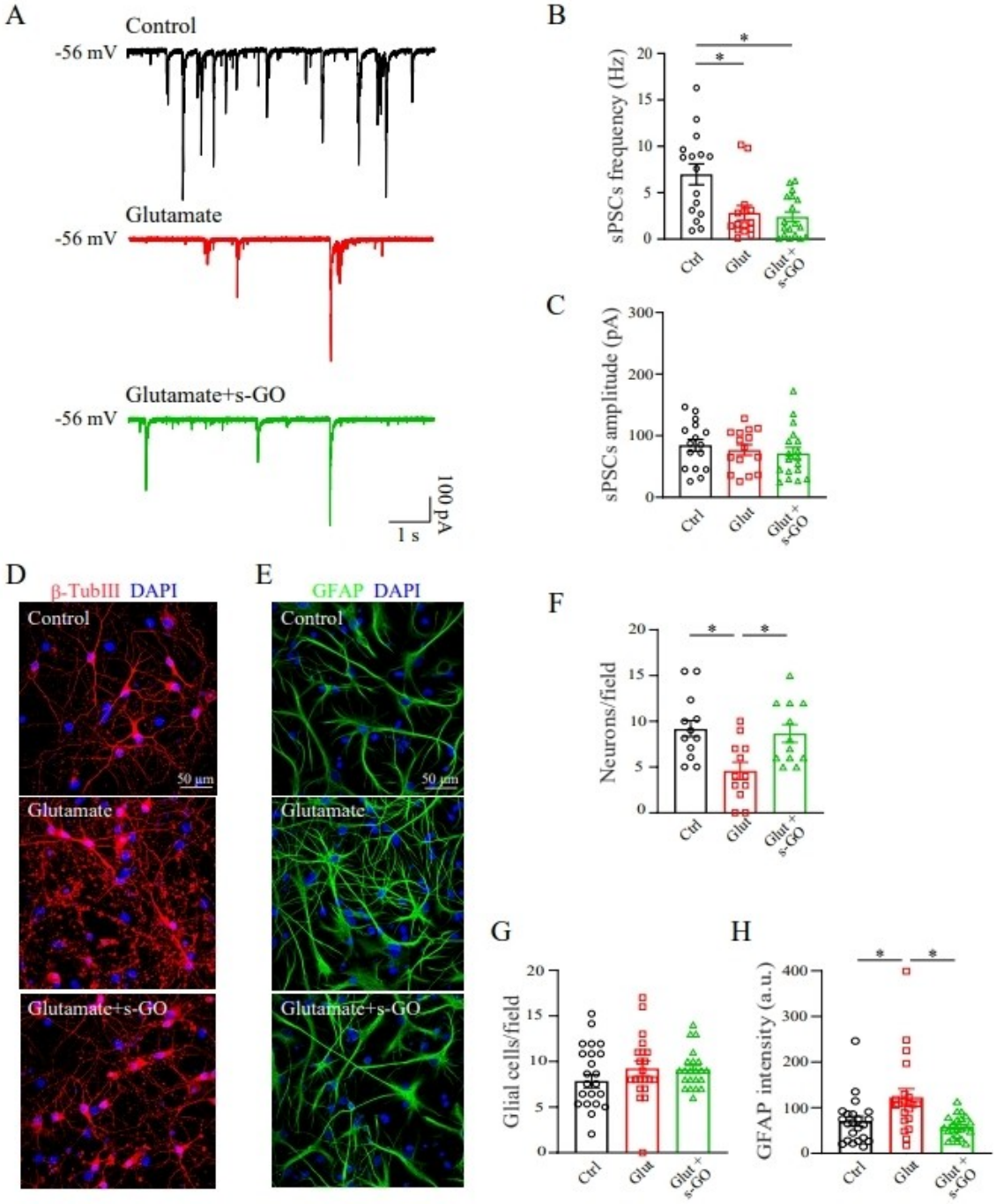

Figure 5. In a model of primary excitotoxicity, s-GO favors neuronal survival and integrity by interfering with synaptic transmission. (A) Representative traces from control (in black), glutamate (in red) and glutamate + s-GO treated cells (in green). Bar plots of sPSCs frequency (B) and amplitude (C). N = 16 in control, N = 15 in glutamate and N = 18 in glutamate + s-GO treated samples. Data are reported as mean ± SEM, while dots superimposed to the bars correspond to single cell values. Magnifications of representative confocal microscopy images obtained from cultures in control condition and exposed to glutamate with or without s-GO (10 μg/mL), immunostained for the neuronal and glial markers β-tubulin III (in red, D) or GFAP (in green, E). In blue cell nuclei staining for DAPI. Note that glutamate application induced a loss in neuronal integrity and glial over-reactivity that were restored by s-GO treatment. Scale bar 50 μm. Bar plots showing the number of neurons with intact neurites (F), the number of GFAP-positive glial cells (G) and the mean GFAP fluorescence intensity (H). Data are reported as mean ± SEM, while dots superimposed to the bars correspond to the single field values. For β-tubulin III staining, N = 22 in control and glutamate + s-GO treated samples and N = 21 for glutamate treated ones, for GFAP staining. *$P < 0.05$.

activity after 24 hours from s-GO treatment, we observed a statistically significant decrease ($P < 0.05$) in the frequency of sPSCs respect to that of the untreated controls (from 0.76 ± 0.22 Hz to 0.28 ± 0.14 Hz, control vs s-GO; Supplementary Figure S2A,B), with no changes in sPSCs amplitudes (81 ± 9 pA and 67 ± 7 pA, control and s-GO respectively, Supplementary Figure S2C), or in neuronal and glial densities or glial reactivity ($P > 0.05$; Supplementary Figure S2D,E,F,G,H). This experiment, in-

dicating that in control s-GO downregulated synaptic activity as expected,[10,12,13,14] suggested that similarly, when glutamate-treated cultures were co-incubated with s-GO, the detected reduction in synaptic activity was due to the nanoparticle modulation, regardless the preserved network size.

We further assessed, 24 hours after the treatments, cell morphology and integrity through immunostaining for the neuronal marker β-tubulin III.[43] In Figure 5D control neurons are characterized by multiple neurites extending from the soma and forming a tangled network. Conversely, upon excitotoxicity a massive loss in neuronal integrity was observed, resulting in only few cells displaying projecting neurites. In each imaged field, we quantified the number of neurons presenting intact neurites extending $\geq 10\,\mu m$ from the cell body. These were decreased from 9 ± 1 neurons/field in control to 5 ± 1 neurons/field in glutamate treated samples (Figure 5F; $P < 0.05$). In cultures co-treated with glutamate and s-GO, neurites were similar to controls, as the number of neurons/field with intact neurites was 9 ± 1 (for glutamate vs glutamate + s-GO, $P < 0.05$, Figure 5F).

In parallel experiments, we evaluated also glial density and reactivity, by staining the cultures for the astrocyte marker GFAP (Figure 5E). While we found no changes in GFAP-positive cell densities among the different conditions (8 ± 1 glial cells/field in control, 9 ± 1 glial cells/field in glutamate treated samples and 9 ± 1 cells/field in glutamate + s-GO treated ones, Figure 5G), GFAP intensity was enhanced by glutamate treatment from 70 ± 9 a.u. in control to 123 ± 19 a.u. in glutamate treated samples (Figure 5H). Additionally, s-GO co-application reverted GFAP reactivity at control level (58 ± 5 a.u. in glutamate + s-GO treated samples, Figure 5H; for control vs glutamate and glutamate vs glutamate + s-GO, $P < 0.05$).

In sum, these experiments confirmed the s-GO protective action, during excitotoxicity. As suggested by the electrophysiological measures, we hypothesize that s-GO, via downregulation of glutamate release,[10,12,13,14] prevents dysregulated glutamatergic activity and protect neuronal survival during glutamate overload.

s-GO modulation of glutamatergic synapses has been reported both *in vitro* and *in vivo*,[10,12,13] including pathological conditions characterized by dysfunctional synaptic plasticity.[14] In this work, we report that s-GO efficiently counteracted neuronal cell death which follows excitotoxicity *in vitro*.

We first focused on ischemic stroke, since the pathogenic cascade leading to cell death includes the excitotoxic process.[16,17,19,44] In this framework, *in vitro* models of ischemia[25] allow to dissect out in a simplified and accessible setting s-GO effects on neurons during excitotoxicity.

In our model, excitotoxicity is secondary to OGD, thus mimicking closely the sequence of pathogenic events occurring *in vivo*[25] and allowing to test the impact of s-GO on cell damage. In this paradigm, we observed that the nanomaterial applied in a therapeutic fashion after OGD (i.e. after the stroke), could prevent cell damage, even more efficiently than the GlutRs antagonists cocktail.

To focus on glutamate-mediated pathways, we reproduced excitotoxicity by exogenous glutamate exposure[20] during which the s-GO was co-applied. This model allowed to infer the mechanisms through which s-GO, by downregulating the activity of glutamatergic synapses, counteracted excitotoxic damage.

s-GO prevented the excitotoxic cell death and this protective action was supposedly mediated by s-GO downregulation of the neurotransmitter release,[10,12,13,14] which is augmented by exogenous glutamate.[40] We propose that the decreased synaptic activity following glutamate exposure emerges mostly from the reduction in circuit size due to neurons death,[41] as supported by the immunostainings, and the measured membrane passive values rule out changes in the membrane potential. s-GO reduced PSCs frequency may instead reflect, the nanomaterial induced downregulation in glutamate-mediated neurotransmission,[10,12,13,14] ultimately protecting neurons from escalating excitotoxicity damage.

Excitotoxicity triggered by exogenous glutamate induced glial over-reactivity, while no glial alterations were detected in OGD. This might be due to the mild OGD paradigm used, but we cannot exclude that the timeline of our histological analysis precluded the characterization of a later glial involvement in the secondary excitotoxic cascade.[33]

The GFAP intensity increase in response to excitotoxicity is a hallmark of neuroinflammation.[45,46] The s-GO ability to downregulate reactive resident glial cells could be a direct effect on astrocytes, namely not mediated by the reduced excitotoxicity. This would be in agreement with our recent study,[22] reporting s-GO downregulation of neuroinflammatory activated astrocytes with s-GO preventing neuronal damage via multiple mechanisms.

Conclusions

Our findings indicate that, by targeting the exceeding presynaptic glutamate release characterizing excitotoxicity, s-GO might be used for the development of alternative therapeutic strategies against excitotoxicity pathogenic mechanisms. Although several studies supported the *in vitro* and *in vivo* biocompatibility of s-GO,[10–14,22,48-50] further investigations are required to support the translation of the nanomaterial in clinical research. These will include the assessment of s-GO long term effects on nervous tissue to evaluate additional impact on glial cells, the therapeutic potential of the nanomaterial on preclinical models of ischemic stroke and s-GO toxicological assessment in course of neuropathologies.

Experimental Section

Synthesis and characterization of s-GO. Biological-grade s-GO material was synthesized in house from graphite powder (Sigma Aldrich, UK) by the modified Hummers method already described under endotoxin-free conditions.[21,51] The specific batch for the s-GO material used in this study was fully characterized and the detailed information for the characterization can be found in.[22]

Materials used for neurobiology experiments. All materials were bought from Sigma-Aldrich company if not differently stated.

Preparation of rat dissociated hippocampal cultures. Dissociated hippocampal cultures were prepared from 2 to 3 days postnatal (P2 – P3) Wistar rats. All procedures were done in agreement with the Italian law (decree 26/14) and the EU guidelines (2007/ 526/CE and 2010/63/UE). The animal use was authorized by the Italian Ministry of Health (authorization number: 22DAB.NYQA) and approved by the local veterinary authorities. Once isolated, hippocampi were treated by enzymatic and mechanical digestion following a procedure describe elsewhere.[52] The obtained cells were seeded on poly-L-ornithine-coated glass coverslips (24×12 mm2, Kindler, EU) at a density of 150,000 cells/mL. Neuronal cultures were maintained in stable conditions (37 °C, 5% CO2) in Neurobasal-A Medium (Gibco) supplemented with 10 mM GlutaMAX (Gibco), 2% B27 supplement (Life Technologies, no. 17504044), and 500 nM gentamycin and replaced after 3 days with fresh medium. Cultures were used for experiments in the second week of differentiation *in vitro*.

OGD treatment. Dissociated hippocampal cultures were exposed to an OGD treatment, according to previous literature.[25] Briefly, neurobasal culturing medium was removed and replaced by 2 mL of sterile OGD medium, lacking glucose and composed as follows (in mM): 130 NaCl, 5.4 KCl, 1.8 $CaCl_2$, 26 $NaHCO_3$, 0.8 $MgSO_4 \cdot 7H_2O$, 1.18 NaH_2PO_4. Cell cultures were transferred to a hypoxic chamber, fabricated by SISSA mechatronic facility, equipped with a pressure lid and an inlet and outlet tubes with respective valves and flushed by a gas mixture consisting of 95% N2 and 5% CO2 for 5 min at 15 L/min. Next, the valves were closed and the chamber was placed in a humidified incubator (37 °C) for 55 minutes. After OGD treatment (lasting overall 1 hour), cell cultures were taken from the chamber and the OGD medium was replaced with the previous culturing medium. The control cells did not undergo to any medium change and were maintained in stable conditions (37 °C, 5% CO_2) for the same time of OGD exposure.

In cultures treated with s-GO after OGD, the nanomaterial was added to the culturing medium at the concentration of 10 μg/mL for 24 hours. The selected concentration of nanomaterial was in the range of those reported in literature to exert effects on neuronal activity without cytotoxicity in culture.[10,14] At the end of the incubation, the medium was replaced with fresh one.

Primary damage model. Under a biological hood, glutamate (L-Glutamic acid potassium salt monohydrate, stock solution 10 mM) was added to culturing medium at the final concentration of 40 μM. Then cultures were incubated at 37 °C for 30 minutes. Glutamate concentration and incubation time were in the range of those reported in literature to induce a significant increase in cell death after 24 hours from the exposure.[20] For s-GO treatments, cultures were incubated with glutamate (40 μM) and s-GO (10 μg/mL) simultaneously. At the end of the incubation time, the medium was washed out and replaced with fresh culturing medium for the following 24 hours.

PI based necrosis assay. PI is a highly polar (not lipidic permeant) fluorescent dye used to assess neuronal death.[25] Applied to cultures together with the NucBlue dye, a cell-permeant nuclear staining, can be exploited to calculate the percentage of necrotic cells in the preparation. Under a chemical hood, the staining solution was prepared adding PI at the final concentration of 1 μg/mL and one drop of NucBlue (NucBlue™ Live ReadyProbes™ Reagent, R37605-Invitrogen™) to the extracellular physiological solution composed (in mM) as follows: 150 NaCl, 4 KCl, 1 $MgCl_2$, 2 $CaCl_2$, 10 HEPES, 10 glucose, pH 7.4. Next, the culture medium was removed from the petri dishes and cells were washed four times with the extracellular solution. Cells were treated with the staining solution for 20 minutes. After mounting the samples on a glass slide (in staining solution), images (3 fields/coverslip) were acquired with a Nikon C2 confocal microscope with a 20X objective (NA 0.50). The analysis was performed offline using the image-processing CellCounting plug-in of Fiji software. Necrotic cells were quantified as percentage of total number of the NucBlue positive cells present in each field.

For the OGD model, two sets of experiments were carried out and for each the number of cells positive to NucBlue were similar among the different conditions. In the first set of experiments, these were 148 ± 11 in control, 171 ± 11 in OGD and 154 ± 11 in OGD + GlutRs antagonists treated samples ($P > 0.05$), while in second one these were 80 ± 4 in control, 81 ± 4 in OGD and 85 ± 4 in OGD + s-GO treated samples ($P > 0.05$).

For the primary damage model, the total number of NucBlue positive cells/field was unchanged among the different experimental conditions (364 ± 20 cells/field in untreated control, 358 ± 24 cells/field in glutamate treated samples and 379 ± 29 cells/field in glutamate + s-GO treated samples, $p > 0.05$).

Immunofluorescence labelling. Hippocampal cells were washed in phosphate buffered saline (PBS) solution and then fixed with 4% paraformaldehyde (PFA) for 20 min at room temperature (RT). Cells were permeabilized with 3% Triton X-100 and blocked with 5% NGS in PBS for 60 min at RT, and then incubated in PBS with 5% FBS and primary antibodies for 60 min. The primary antibodies used were mouse monoclonal anti-NeuN (Millipore, 1:500 dilution), rabbit polyclonal anti-β-tubulin III (Sigma, 1:500 dilution), mouse polyclonal anti-GFAP (Sigma, 1:500 dilution). After the primary incubation and PBS washes, cells were incubated for 60 min with the secondary antibodies Alexa Fluor 488 goat anti-mouse (Invitrogen, no. A-11001; dilution 1:500), Alexa Fluor 594 goat anti-rabbit (Invitrogen, no. A-11008; dilution 1:500). DAPI (Invitrogen, no. D1306; dilution 1:500) was used to stain the nuclei. Samples were mounted in anti-fade medium Fluoromont-G™ (Invitrogen™ 00495802) on 24 x 60 mm^2 glass slide (0.13-0.17 mm thick, Menzel-Gläser). Image acquisition was performed using a confocal microscope (Nikon C2-si Laser Scanning Confocal Microscope) with 20x (0.50 NA) and 40x (0.75 NA) air objectives (Z-stacks were acquired every 500 nm).

Mitochondrial imaging. Cultures were treated with glutamate in the presence or absence of s-GO and with s-GO alone as supramentioned and compared with untreated (control) ones. Cells were labelled with MitoTracker™ Red CM–XRos (2 μM, M7512; Invitrogen; Thermo Fisher Scientific, Inc.), according to,[53] together with NucBlue dye, at 37°C in a humidified 5% CO_2 atmosphere for 24 hours. Then cells were rinsed twice with PBS, mounted on a glass slide and imaged at the confocal microscope with a 40X objective. The number of cells co-stained for MitoTracker Red CM–XRos and NucBlue was manually counted using Fiji software.

Electrophysiological recordings. Neuronal activity was recorded from hippocampal cultures through single cell patch clamp technique. Voltage clamp whole-cell recordings were performed at RT with pipettes (3–5 MΩ) containing (in mM): 120 K gluconate, 20 KCl, 2 MgCl2, 10 EGTA, 10 HEPES, 2 Na2ATP, pH 7.3. The extracellular solution was the one used for PI based assay. Cultures were mounted on a chamber and visualized with an inverted microscope (Nikon Eclipse Ti-U). During experiments, neurons were continuously perfused with an extracellular solution through a gravity-based perfusion system at a rate of 1 mL/min. Recordings were performed through a Multiclamp 700B patch amplifier (Axon CNS, Molecular Devices) with a sampling rate of 10 kHz. Data were acquired using a pClamp 10.3 software (Molecular Devices LLC, USA). Capacitative transients due to the recording pipette were compensated. All the recorded neurons were characterized by a series resistance less than 1/10 of the membrane resistance and it

remained stable for the entire duration of the recording. In order to measure the input resistance and cell capacitance, a stimulation protocol was applied while the cell was clamped close to the resting membrane potential (−56 mV). It consisted in 100 ms long lasting depolarizing steps of voltage (10 mV of amplitude), repeated 10 times. For single cells, the currents elicited by these stimulations were recorded and averaged. The input resistance was calculated according to Ohm's law: $\Delta V = R\,\Delta I$ (ΔV: applied pulse; R: resistance; ΔI: current). The membrane capacitance was calculated as the integral in time of the capacitive transient (elicited by the voltage step), divided for the amplitude of the applied ΔV. Resting membrane potential was measured in current clamp in $I = 0$. These passive membrane properties, used as indicators of neuronal degree of maturation and health,[54,55,56] were analysed offline with the software Clampfit 10.6.

Upon the different treatments, no significant difference between the experimental groups were observed in membrane capacitance (control: 73 ± 3 pF, glutamate: 62 ± 3 pF, glutamate + s-GO: 63 ± 4 pF), input resistance (control: 456 ± 65 MΩ, glutamate: 587 ± 47 MΩ, glutamate + s-GO: 533 ± 56 MΩ) and resting membrane potential (control: −60 ± 2, glutamate: −60 ± 1, glutamate + s-GO: −55 ± 2 mV). This indicated that recordings were performed from three groups of neurons presenting homogeneous properties.

Recordings of spontaneous postsynaptic activity were performed at a holding potential of −56 mV (not corrected for liquid junction potential, which was −14 mV). For each trace, amplitude and frequency of sPSCs were evaluated offline with Axograph 1.4.4 event detection software. This exploits a detection algorithm based on sliding templates to separate glutamatergic fast decaying (~4 ms) and GABAergic slow decaying (~25 ms) postsynaptic currents on the basis of their different decay times. In control cultures, 74% of sPSCs were of glutamatergic nature.

Statistical analysis. All the statistical analyses were carried out using GraphPad Prism 8. The Gaussian distribution of data was assessed through Shapiro-Wilk test. If all the data compared in one set of experiments resulted parametric, next statistically significant differences were assessed by one way ANOVA test, using Tukey's Multiple Comparisons as post hoc test. In opposition, if data were not distributed as in a Gaussian distribution, non-parametric analysis was used (Kruskal-Wallis test was performed and Dunn's Multiple Comparison was used as post hoc test). p values were considered statistically significant when minor than 0.05. Data are reported as mean with the standard error of the mean (SEM). N is the number of cells or analyzed fields.

Acknowledgements

This work received funding from the European Union Horizon 2020 Research and Innovation Programme under Grant Agreement No. GrapheneCore3 (881603). We would like to acknowledge Dr. Michelle Ntola for the synthesis of the specific GO batch used in this work and Dr. Luis Miguel Arellano and Angeliki Karakasidi for their contributions to the full characterization of the s-GO material. The ICN2 has been supported by the Severo Ochoa Centres of Excellence programme [SEV-2017-0706] and is currently supported by the Severo Ochoa Centres of Excellence programme, Grant CEX2021-001214-S, both funded by MCIN/AEI/10.13039.501100011033. We are grateful to Marco Gigante (SISSA Mechatronic lab) for the help in setting up the apparatus for OGD, to Raffaele Casani and Mario Fontanini for technical support for cell cultures and to Prof. Gabriele Baj for his support regarding mitochondria labelling.

Conflict of Interests

The authors declare no conflict of interest.

Data Availability Statement

The data that support the findings of this study are available from the corresponding author upon reasonable request.

Keywords: graphene oxide · excitotoxicity · *in vitro* ischemic stroke · nanomedicine · glutamatergic synapses

[1] Y. Yang, A. M. Asiri, Z. Tang, D. Du, Y. Lin, *Mater. Today* **2013**, *16 (10)*, 365–373.
[2] K. Kostarelos, K. S. Novoselov, *Science* **2014**, *344 (6181)*, 261–263.
[3] A-I. Lazăr, K. Aghasoleimani, A. Semertsidou, J. Vyas, A-L. Roşca, D. Ficai, A. Ficai, *Nanomaterials* **2023**, *13*, 1092.
[4] K. E. Kitko, Q. Zhang, *Front. Neurol. Neurosci.* **2019**, *13*, 26.
[5] M. K. Akbari, N. S. Lopa, M. Shahriari, A. Najafzadehkhoee, D. Galusek, S. Zhuiykov, *J. Funct. Biomater.* **2023**, *14*, 35.
[6] B. Zhang, Y. H. Koh, R. B. Beckstead, V. Budnik, B. Ganetzky, H. J. Bellen, *Neuron* **1998**, *21*, 1465–75.
[7] K. R. Smith, K. J. Kopeikina, J. M. Fawcett-Patel, K. Leaderbrand, R. Gao, B. Schürmann, K. Myczek, J. Radulovic, G. T. Swanson, P. Penzes, *Neuron* **2014**, *84*, 399–415.
[8] E. Pchitskaya, I. Bezprozvanny, *Front. Synaptic Neurosci.* **2020**, *12*, 31.
[9] G. Cellot, A. Franceschi Biagioni, L. Ballerini, *Pediatr. Res.* **2022**, *92*, 71–79.
[10] R. Rauti, N. Lozano, V. León, D. Scaini, M. Musto, I. Rago, F. P. Ulloa Severino, A. Fabbro, L. Casalis, E. Vázquez, K. Kostarelos, M. Prato, L. Ballerini, *ACS Nano* **2016**, *10*, 4459–71.
[11] N. Secomandi, A. Franceschi Biagioni, K. Kostarelos, G. Cellot, L. Ballerini, *Nanomedicine* **2020**, *26*, 102174.
[12] G. Cellot, S. Vranic, Y. Shin, R. Worsley, A. F. Rodrigues, C. Bussy, C. Casiraghi, K. Kostarelos, J. R. McDearmid, *Nanoscale Horiz.* **2020**, *5*, 1250–1263.
[13] R. Rauti, M. Medelin, L. Newman, S. Vranic, G. Reina, A. Bianco, M. Prato, K. Kostarelos, L. Ballerini, *Nano Lett.* **2019**, *19*, 2858–2870.
[14] A. Franceschi Biagioni, G. Cellot, E. Pati, N. Lozano, B. Ballesteros, R. Casani, N. C. Coimbra, K. Kostarelos, L. Ballerini, *Biomaterials* **2021**, *271*, 120749.
[15] A. Granzotto, L. M. T. Canzoniero, S. L. Sensi, *Front. Mol. Neurosci.* **2020**, *13*, 600089.
[16] B. Puig, S. Brenna, T. Magnus, *Int. J. Mol. Sci.* **2018**, *19*, 2834.
[17] M. Szatkowski, D. Attwell, *Trends Neurosci.* **1994**, *17*, 359–365.
[18] C. Iadecola, J. Anrather, *Nat. Med.* **2011**, *17*, 796.
[19] S. G. Daniele, G. Trummer, K. A. Hossmann, Z. Vrselja, C. Benk, K. T. Gobeske, D. Damjanovic, D. Andrijevic, J. S. Pooth, D. Dellal, F. Beyersdorf, N. Sestan, *Nat. Rev. Neurosci.* **2021**, *22*, 553–572.
[20] A. P. Simões, C. G. Silva, J. M. Marques, D. Pochmann, L. O. Porciúncula, S. Ferreira, J. P. Oses, R. O. Beleza, J. I. Real, A. Köfalvi, B. A. Bahr, J. Lerma, R. A. Cunha, R. J. Rodrigues, *Cell Death Dis.* **2018**, *9*, 297.
[21] A. F. Rodrigues, L. Newman, N. Lozano, S. P. Mukherjee, B. Fadeel, C. Bussy, K. Kostarelos, *2D Mater.* **2018**, *5 (3)*, 035020.
[22] G. Di Mauro, R. Amoriello, N. Lozano, A. Carnasciali, D. Guasti, M. Becucci, G. Cellot, K. Kostarelos, C. Ballerini, L. Ballerini, *ACS Nano* **2023**, *17*, 1965–1978.
[23] M. P. Goldberg, D. W. Choi, *J. Neurosci.* **1993**, *13 (8)*, 3510–24.
[24] R. Wang, X. Zhang, Y. Fan, Y. Shen, W. Hu, Z. Chen, *PLoS One* **2012**, *7 (5)*, e37574.
[25] C. I. Tasca, T. Dal-Cim, H. Cimarosti, *Methods Mol. Biol.* **2015**, *1254*, 197–210.

[26] J. Zhang, L. Huang, X. Shi, L. Yang, F. Hua, J. Ma, W. Zhu, X. Liu, R. Xuan, Y. Shen, J. Liu, X. Lai, P. Yu, *Aging (Albany NY)* **2020**, *12 (23)*, 24270–24287.
[27] M. I. Cuartero, J. de la Parra, A. Garcia-Culebras, I. Ballesteros, I. Lizasoain, M. A. Moro, *Curr. Pharm. Des.* **2016**, *22*, 1060–1073.
[28] S. Y. Lee, J. H. Kim, *J. Physiol.* **2015**, *593 (13)*, 2793–806.
[29] A. L. Andrade, D. J. Rossi, *J. Physiol.* **2010**, *588 (9)*, 1499–1514.
[30] K. Kuboyama, H. Harada, H. Tozaki-Saitoh, M. Tsuda, K. Ushijma, K. Inoue, *J. Cereb. Blood Flow Metab.* **2011**, *31 (9)*, 1930–1941.
[31] D. W. Choi, *J. Neurobiol.* **1992**, *23 (9)*, 1261–76.
[32] L. C. Crowley, A. P. Scott, B. J. Marfell, J. A. Boughaba, G. Chojnowski, N. J. Waterhouse, *Cold Spring Harb. Protoc.* **2016**, *2016 (7)*, 10.1101/pdb.prot087163.
[33] Y. Du, W. Wang, A. D. Lutton, C. M. Kiyoshi, B. Ma, A. T. Taylor, J. W. Olesik, D. M. McTigue, C. C. Askwith, M. Zhou, *Exp. Neurol.* **2018**, *303*, 1–11.
[34] W. Duan, Y. P. Zhang, Z. Hou, C. Huang, H. Zhu, C. Q. Zhang, Q. Yin, *Mol. Neurobiol.* **2016**, *53*, 1637–1647.
[35] E. M. Hol, M. Pekny, *Curr. Opin. Cell Biol.* **2015**, *32*, 121–130.
[36] J. Kapuscinski, *Biotech. Histochem.* **1995**, *70 (5)*, 220–233.
[37] C. Y. Li, X. Li, S. F. Liu, W. S. Qu, W. Wang, D. S. Tian, *Neurochem. Int.* **2015**, *83*, 9–18.
[38] D. Schiffer, M. T. Giordana, A. Migheli, G. Giaccone, S. Pezzotta, A. Mauro, *Brain Res.* **1986**, *374 (1)*, 110–118.
[39] Doble A, *Pharmacol. Ther.* **1999**, *81*, 163–221.
[40] C. M. Norris, E. M. Blalock, O. Thibault, L. D. Brewer, G. V. Clodfelter, N. M. Porter, P. W. Landfield, *J. Neurophysiol.* **2006**, *96 (5)*, 2488–500.
[41] E. Cohen, M. Ivenshitz, V. Amor-Baroukh, V. Greenberger, M. Segal, *Brain Res.* **2008**, *1235*, 21–30.
[42] J. Simonnet, L. Richevaux, D. Fricker, *Methods Mol. Biol.* **2021**, *2188*, 285–309.
[43] C. D. Katsetos, A. Legido, E. Perentes, S. J. Mörk, *J. Child Neurol.* **2003**, *18*, 851–66.
[44] T. W. Lai, S. Zhang, Y. T. Wang, *Prog. Neurobiol.* **2014**, *115*, 157–88.
[45] P. M. George, G. K. Steinberg, *Neuron* **2015**, *87 (2)*, 297–309.
[46] M. Pekny, M. Pekna, *Physiol. Rev.* **2014**, *94 (4)*, 1077–1098.
[47] H. P. Makarenkova, V. I. Shestopalov, *Front. Plant Physiol.* **2014**, *5*, 63.
[48] D. A. Jasim, C. Ménard-Moyon, D. Bégin, A. Bianco, K. Kostarelos, *Chem. Sci.* **2015**, *6*, 3952–3964.
[49] A. F. Rodrigues, L. Newman, D. Jasim, S. P. Mukherjee, J. Wang, I. A. Vacchi, C. Ménard-Moyon, A. Bianco, B. Fadeel, K. Kostarelos, C. Bussy, *Adv. Sci.* **2020**, *7 (12)*,1903200.
[50] S. P. Mukherjee, A. R. Gliga, B. Lazzaretto, B. Brandner, M. Fielden, C. Vogt, L. Newman, A. F. Rodrigues, W. Shao, P. M. Fournier, M. S. Toprak, A. Star, K. Kostarelos, d K. Bhattacharyaa, B. Fadeel, *Nanoscale* **2018**, *10*, 1180–1188.
[51] S. P. Mukherjee, N. Lozano, M. Kucki, A. E. Del Rio-Castillo, L. Newman, E. Vázquez, K. Kostarelos, P. Wick, B. Fadeel, *PLoS One* **2016**, *11 (11)*, e0166816.
[52] G. Cellot, F. M. Toma, Z. K. Varley, J. Laishram, A. Villari, M. Quintana, S. Cipollone, M. Prato, L. Ballerini, *J. Neurosci.* **2011**, *31*, 12945–53.
[53] Y. Zhang, N. S. Gliyazova, P. A. Li, G. Ibeanu, *Exp. Ther. Med.* **2021**, *21*, 221.
[54] J. S. Carp, *J. Neurophysiol.* **1992**, *68*, 1121–1132.
[55] Y. Gao, L. Liu, Q. Li, Y. Wang, *Neurosci. Lett.* **2015**, *591*, 138–143.
[56] U. Djuric, A. Y. Cheung, W. Zhang, R. S. Mok, W. Lai, A. Piekna, J. A. Hendry, P. J. Ross, P. Pasceri, D. S. Kim, M. W. Salter, J. Ellis, *Neurobiol. Dis.* **2015**, *76*, 37–45.

Manuscript received: June 5, 2023
Accepted manuscript online: September 14, 2023
Version of record online: October 20, 2023